MNRAS **000**, 1–6 (2015) Preprint August 4, 2015 Compiled using MNRAS LATEX style file v3.0

The Brightest Lyα Emitter: Pop III or Black Hole?

A. Pallottini[1⋆], A. Ferrara[1,2], F. Pacucci[1], S. Gallerani[1], S. Salvadori[3], R. Schneider[4], D. Schaerer[5,6], D. Sobral[7,8,9], J. Matthee[9]

[1] *Scuola Normale Superiore, Piazza dei Cavalieri 7, I-56126 Pisa, Italy*
[2] *Kavli IPMU, The University of Tokyo, 5-1-5 Kashiwanoha, Kashiwa 277-8583, Japan*
[3] *Kapteyn Astronomical Institute, Landleven 12, 9747 AD Groningen, The Netherlands*
[4] *INAF, Osservatorio Astronomico di Roma, Via Frascati 33, 00040 Monteporzio Catone, Italy*
[5] *Observatoire de Genève, Departement d'Astronomie, Université de Genève, 51 Ch. des Maillettes, 1290 Versoix, Switzerland*
[6] *CNRS, IRAP, 14 Avenue E. Belin, 31400 Toulouse, France*
[7] *Instituto de Astrofísica e Ciências do Espaço, Universidade de Lisboa, OAL, Tapada da Ajuda, PT1349-018 Lisboa, Portugal*
[8] *Departamento de Física, Faculdade de Ciências, Universidade de Lisboa, Edifício C8, Campo Grande, PT1749-016 Lisbon, Portugal*
[9] *Leiden Observatory, Leiden University, P.O. Box 9513, NL-2300 RA Leiden, The Netherlands*

ABSTRACT

CR7 is the brightest $z = 6.6$ Lyα emitter (LAE) known to date, and spectroscopic follow-up by Sobral et al. (2015) suggests that CR7 might host Population (Pop) III stars. We examine this interpretation using cosmological hydrodynamical simulations. Several simulated galaxies show the same "Pop III wave" pattern observed in CR7. However, to reproduce the extreme CR7 Lyα/HeII1640 line luminosities ($L_{\alpha/\rm HeII}$) a top-heavy IMF and a massive ($\gtrsim 10^7 M_\odot$) Pop III burst with age $\lesssim 2$ Myr are required. Assuming that the observed properties of Lyα and HeII emission are typical for Pop III, we predict that in the COSMOS/UDS/SA22 fields, 14 out of the 30 LAEs at $z = 6.6$ with $L_\alpha > 10^{43.3}$erg s^{-1} should also host Pop III stars producing an observable $L_{\rm HeII} \gtrsim 10^{42.7}$erg s^{-1}. As an alternate explanation, we explore the possibility that CR7 is instead powered by accretion onto a Direct Collapse Black Hole (DCBH). Our model predicts L_α, $L_{\rm HeII}$, and X-ray luminosities that are in agreement with the observations. In any case, the observed properties of CR7 indicate that this galaxy is most likely powered by sources formed from pristine gas. We propose that further X-ray observations can distinguish between the two above scenarios.

Key words: stars: Population III – galaxies: high-redshift – black hole physics

1 INTRODUCTION

The end of the Dark Ages is marked by the appearance of the first stars. Such – Pop III – stars had to form out of a pristine composition (H+He) gas with virtually no heavy elements. Lacking these cooling agents, the collapse had to rely on the inefficient radiative losses provided by H_2 molecules. Mini-halos, i.e. nonlinear dark matter structures with mass $M_h \sim 10^{6-7} M_\odot$ collapsing at high redshift ($z \sim 30$), are now thought to be the preferred sites of first star formation episodes (Yoshida et al. 2006; Turk et al. 2009; Salvadori & Ferrara 2009; Greif et al. 2012; Visbal et al. 2015). Although the Initial Mass Function (IMF) of Pop III stars is largely uncertain, physical arguments suggest that they could have been more massive than present-day (Pop II) stars. Furthermore, the metals produced by Pop III stars polluted the surrounding gas (Bromm et al. 2002; Wise et al. 2012; Xu et al. 2013), inducing a transition to the Pop II star formation mode ("chemical feedback", Schneider et al. 2002, 2006). Metal enrichment is far from being homogeneous, and pockets of pristine gas sustaining Pop III star formation can in principle persist down to $z \simeq 3-4$ (Tornatore et al. 2007; Trenti et al. 2009; Maio et al. 2010; Salvadori et al. 2014; Pallottini et al. 2014a; Ma et al. 2015), yielding Pop III star formation rate (SFR) densities of $\sim 10^{-4} M_\odot {\rm yr}^{-1} {\rm Mpc}^{-3}$, i.e. $\lesssim 1\%$ of the Pop II SFR density at those redshifts.

The search effort for Pop III stars at moderate and high redshifts has become increasingly intense in the last few years (e.g. Kashikawa et al. 2012; Heap et al. 2015). Observationally, a galaxy hosting a recent ($t_\star \lesssim 2$ Myr) Pop III star formation episode should show strong Lyα and He II lines and no metal lines (e.g. Schaerer 2002; Raiter et al. 2010; Kehrig et al. 2015). Until now, no indisputable evidence for Pop III stars in distant galaxies has been obtained, and observations have only yielded upper bounds on Pop III SFR (e.g. Cai et al. 2011; Cassata et al. 2013; Zabl et al. 2015).

⋆ email: andrea.pallottini@sns.it

This situation might dramatically change following the recent observations of CR7 by Sobral et al. (2015, S15 hereafter).

CR7 is the brightest Lyα emitter (LAE) at $z > 6$, and it is found in the COSMOS field (Matthee et al. 2015). Spectroscopic follow-up by S15 suggests that CR7 might host a PopIII-like stellar population. This is based on the astonishingly bright Lyα and He II lines ($L_\alpha \simeq 10^{43.93}$erg s^{-1}, $L_{\rm HeII} \simeq 10^{43.29}$erg s^{-1}) and no detection of metal lines. S15 shows that CR7 can be described by a composite of a PopIII-like and a more normal stellar population, which would have to be physically separated, and that would be consistent with e.g. Tornatore et al. (2007). HST imaging shows that CR7 is indeed composed of different components: 3 separate sub-systems (A, B, C) with projected separations of $\lesssim$ 5kpc. F110W(YJ) and F160W(H) band photometry indicates that clump A might be composed of young (blue) stars, while the stellar populations of B+C are old and relatively red. The observed Lyα and He II lines are narrow (FWHM $\lesssim 200\,{\rm km\,s^{-1}}$ and FWHM $\lesssim 130\,{\rm km\,s^{-1}}$, respectively), disfavoring the presence of an AGN or Wolf-Rayet (WR) stars, which are expected to produce much broader (FWHM $\gtrsim 10^3{\rm km\,s^{-1}}$) lines (e.g. De Breuck et al. 2000; Brinchmann et al. 2008; Erb et al. 2010). S15 concluded that CR7 likely contains a *composite* stellar population, with clump A being powered by a recent Pop III-like burst ($t_\star \lesssim 2\,$Myr), and clumps B+C containing an old ($t_\star \sim 350\,$Myr) burst of Pop II stars with $M_\star \simeq 10^{10}{\rm M}_\odot$, largely dominating the stellar mass of the entire system.

Based on cosmological simulations that follows the simultaneous evolution of Pop II and Pop III stars (Pallottini et al. 2014a, P14 hereafter), we examine the interpretation of CR7 as a Pop III host system and explore its implications. We also propose an alternate explanation, briefly discussed in S15, where CR7 is powered by accretion onto a Direct Collapse Black Hole and suggest further tests.

2 SIMULATION OVERVIEW

We use the ΛCDM cosmological[1] hydrodynamical simulations presented in P14 (see that paper for a comprehensive description), obtained with a customized version of the Adaptive Mesh Refinement code RAMSES (Teyssier 2002) to evolve a $(10h^{-1}$ Mpc$)^3$ volume from $z = 99$ to $z = 4$, with a dark matter mass resolution of $\simeq 5 \times 10^5\,h^{-1}{\rm M}_\odot$, and an adaptive baryon spatial resolution ranging from $\simeq 20\,h^{-1}$ kpc to $\simeq 1\,h^{-1}$ kpc. Star formation is included via sub-grid prescriptions based on a local density threshold. If the star forming cell gas has metallicity below (above) the critical metallicity, $Z_{\rm crit} \equiv 10^{-4}{\rm Z}_\odot$, we label the newly formed stars as Pop III (Pop II). Supernova feedback accounts for metal-dependent stellar yields and return fractions appropriate for the relevant stellar population[2]. The simulated galaxy sample reproduces the observed cosmic SFR (Bouwens et al. 2012; Zheng et al. 2012) and stellar mass density (González et al. 2011) evolution in the redshift range $4 \leqslant z \lesssim 10$, and – as shown in Pallottini et al. (2015) – P14 reproduce the observed the luminosity function at $z = 6$. Additionally, the derived Pop III cosmic SFR density is consistent with current observational upper limits (e.g. Nagao et al. 2008; Cai et al. 2011; Cassata et al. 2013). To allow a direct comparison with CR7 we will concentrate on the analysis of the $z \simeq 6$ simulation output.

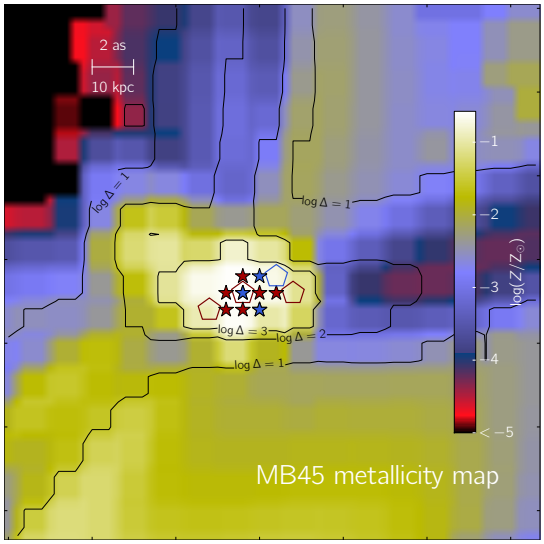

Figure 1. Metallicity (Z) map centered on the simulated galaxy MB45. Pop II locations are marked with filled stars, for recent (blue, $t_\star \lesssim 2$ Myr) and old (red) formation events, respectively. Locations of the recent (old) Pop III burst are shown by the open blue (red) pentagons. Overdensity ($\log\Delta = 1, 2,$ and 3) contours are plotted with black lines. The scale is indicated in arcsecond and kpc.

2.1 Pop III-hosting galaxies

As noted in S15, the interpretation of CR7 fits in the "Pop III wave" scenario suggested by Tornatore et al. (2007). As an example of Pop III wave in action, we show the case of "MB45", a simulated P14 galaxy with total stellar mass $M_\star = 10^{7.9}{\rm M}_\odot$. In Fig. 1, we plot the metallicity (Z) and overdensity (Δ) map around MB45. The star formation history in MB45 starts with a Pop III event. These stars explode as supernovae enriching with metals the central regions of MB45. As a result, star formation there continues in the Pop II mode, while in the less dense external regions, not yet reached by the metal-bearing shocks, Pop III stars can still form. The process repeats until the unpolluted regions have densities exceedingly low to sustain star formation.

The total (i.e. old+young stars) Pop III mass in MB45 is $M_3 \simeq 10^{6.8}{\rm M}_\odot$; about 20% of this stellar mass formed in a recent burst (age $t_\star \lesssim 2$ Myr). The total stellar mass ($M_\star \simeq 10^8 M_\odot$) of MB45 is dominated by Pop II stars produced at a rate ${\rm SFR}_2 \simeq 0.5\,{\rm M}_\odot\,{\rm yr}^{-1}$. Thus, while MB45

[1] We assume a ΛCDM cosmology with total matter, vacuum and baryonic densities in units of the critical density $\Omega_\Lambda = 0.727$, $\Omega_{dm} = 0.228$, $\Omega_b = 0.045$, Hubble constant ${\rm H}_0 = 100$ h km s^{-1} Mpc^{-1} with h $= 0.704$, spectral index $n = 0.967$, $\sigma_8 = 0.811$ (Larson et al. 2011).

[2] While in P14 we explore different types of IMF for Pop III, here we show results assuming a Pop II-like Salpeter IMF. It is to note that our simulations suggests that the Pop III SFR seems almost independent from the IMF (see in particular Fig. 14 in P14).

formation activity proceeds in the Pop III wave mode and resembles that of CR7, the physical properties of MB45 and CR7 are different, because of the 2 orders of magnitude difference in total stellar mass. A direct comparison between the PopIII-PopII separation in CR7 (projected $\simeq 5$ kpc) and MB45 (10 kpc, projected $\lesssim 5$ kpc), although fairly consistent, might not be very meaningful due to the different mass of the two systems. This is because the separation depends on the mass-dependent metallicity profile in galaxy groups (see Fig.1 in Pallottini et al. 2014b). However, we note that our current simulated volume is simply to small to be able to directly recover sources such as CR7, with volume densities of $\sim 10^{-6}\,\mathrm{Mpc}^{-3}$.

The simulated volume contains many galaxies hosting Pop III star formation, whose number density (n_{gal}) as a function of their total stellar mass ($M_\star$) is shown in Fig. 2, along with their Pop III mass (M_3). Pop III stars are found preferentially in low-mass systems $M_\star \lesssim 10^{6.5}\mathrm{M}_\odot$, that typically form these stars in a series of a few $M_3 \simeq 10^6\mathrm{M}_\odot$ bursts[3], before Pop III formation is quenched by chemical feedback.

Note that all larger galaxies, $M_\star \gtrsim 10^7\mathrm{M}_\odot$, contain some Pop III component inherited from progenitor halos. We can then regard M_3 calculated by summing old and young Pop III stars as a solid upper bound to the total Pop III mass produced during the galaxy lifetime. The size of the simulation volume, dictated by the need of resolving the very first star-forming halos, is too small to fairly sample the mass function of galaxies with $M_\star \gtrsim 10^9\mathrm{M}_\odot$ and more massive. To make predictions in this high-mass range, we slightly extrapolate the simulated trends of n_{gal} and M_3 (lines in Fig. 2). We caution that such extrapolation might imply uncertainties.

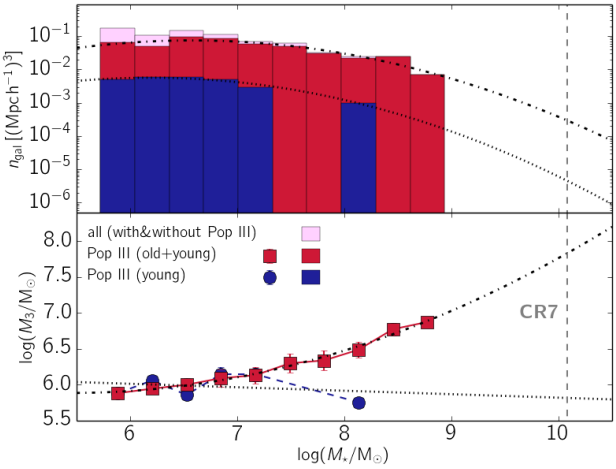

Figure 2. Upper panel: Number density (n_{gal}) of simulated galaxies as a function of their total stellar mass ($M_\star = M_2 + M_3$) for: (i) all galaxies (pink bar), (ii) galaxies with old+young Pop III stars (red bars), (iii) galaxies with a young Pop III component (blue bars). All quantities are averaged on $\log(\Delta M/\mathrm{M}_\odot) \simeq 0.3$ bins. Black dot-dashed and dotted lines correspond to the best-fit analytical extrapolation of n_{gal}. **Lower panel**: Mass of Pop III (M_3) in composite galaxies considering young (blue circle) and old+young (red squares) stars. In both panels the vertical dashed line indicates the value of $M_\star$ for CR7 as inferred by SED fitting (see Sec. 2.2).

2.2 Lyα and He II emission

We label as *pure* (*composite*) galaxies whose emission is produced by Pop II only (Pop II+Pop III) stars. For a pure galaxy, the Lyα line luminosity is (e.g. Dayal et al. 2008):

$$L_\alpha^{\mathrm{pure}} = 2.8\times10^{42} A_\alpha\,\mathrm{SFR}_2\ \mathrm{erg\,s^{-1}}\,, \qquad (1a)$$

where A_α is an attenuation factor that accounts for both internal (interstellar medium) absorption and intergalactic medium transmissivity; Pop II SFR is expressed in $\mathrm{M}_\odot\mathrm{yr}^{-1}$ and to relate this to the $M_\star$ we assume $\mathrm{SFR}_2/M_\star = \mathrm{sSFR} \simeq 2.5\,\mathrm{Gyr}^{-1}$, consistent with our simulations and observations (Daddi et al. 2007; McLure et al. 2011; González et al. 2011, see Sec. 3). Pure galaxies have no He II emission. For a composite galaxy, the Lyα emission is the sum of the contributions from Pop II and Pop III components:

$$L_\alpha^{\mathrm{comp}} = L_\alpha^{\mathrm{pure}} + A_\alpha l_3^\alpha M_3\,, \qquad (1b)$$

where l_3^α is the Pop III Lyα line luminosity per unit stellar mass[4]. Analogously, the He II emission is given by

$$L_{\mathrm{HeII}} = l_3^{\mathrm{HeII}} M_3\,, \qquad (1c)$$

where l_3^{HeII} is the Pop III He II luminosity per unit stellar mass. Both l_3^α and l_3^{HeII} depend on the IMF and burst age, $t_\star$. We adopt the Pop III models by Schaerer (2002) and Raiter et al. (2010), and we use a Salpeter IMF (power-law slope $\alpha = -2.35$), with variable lower (m_{low}) and upper (m_{up}) limits. As long as $m_{up} \gtrsim 10^2\mathrm{M}_\odot$, the results are very weakly dependent on the upper limit, which we therefore fix to $m_{up} = 10^3\mathrm{M}_\odot$, leaving m_{low} as the only free-parameter.

As noted by S15, to reproduce CR7 L_α and L_{HeII} with Pop IIIs, a mass of $M_3 \simeq 10^{7-9}\mathrm{M}_\odot$ *newly-born* ($t_\star \lesssim 2-5$ Myr) stars is required, depending on the IMF. Such a large amount of *young* Pop III stars is contained in none of P14 galaxies and it is not predicted by the adopted analytical extrapolation (see Fig. 2). Thus none of the simulated composite galaxies would reproduce CR7 line emission. However, it is possible that CR7 might have experienced a more vigorous Pop III star formation burst as a result of a very rare event – e.g. a recent major merger – not frequent enough to be captured in our limited box volume. As an estimate we adopt the value of M_3 resulting from the sum of all (old+young) Pop III stars formed in our galaxies.

Under this hypothesis, we can fix m_{low}, by using the zero age main sequence (ZAMS) tracks ($t_\star = 0$). By SED fitting, S15 shows that CR7 Pop II stellar mass (completely contained in clumps B+C) is likely $M_\star \simeq M_2 \simeq 10^{10}\mathrm{M}_\odot$. From the lower panel of Fig. 2, we find that this mass corresponds to a Pop III mass of $M_3 \sim 10^{7.5}\mathrm{M}_\odot$. From Pop III SED fits of region A S15 estimate $M_3 \sim 10^7\mathrm{M}_\odot$. As these stars must be located in CR7 clump A, whose He II luminosity is $L_{\mathrm{HeII}} = 10^{43.3}\mathrm{erg\,s^{-1}}$, eq. 1c requires that $l_3^{\mathrm{HeII}} = 10^{35.5}\mathrm{erg\,s^{-1}\,M_\odot^{-1}}$. In turn this entails a top-heavy IMF with $m_{low} = 6.7\,\mathrm{M}_\odot$.

Having fixed the IMF, we can readily derive the predicted Pop III contribution to the Lyα emission; this turns out to be $l_3^\alpha = 10^{36.7}\mathrm{erg\,s^{-1}\,M_\odot^{-1}}$. CR7 has an observed

[3] We refer to App. A of P14 for possible resolution effects.
[4] We are implicitly assuming that Pop III stars form in a burst, an assumption justified by the analysis presented in Sec. 2.1.

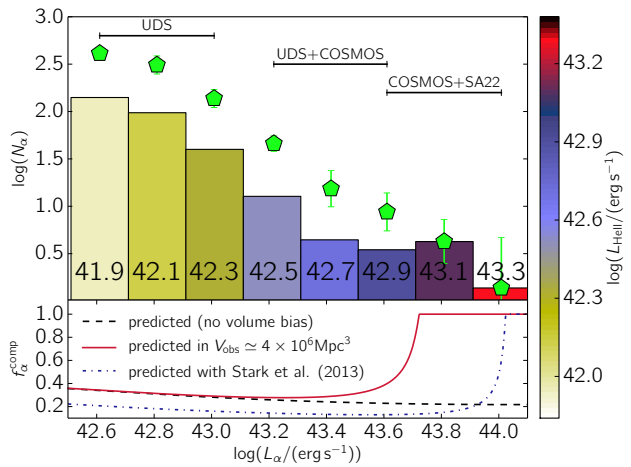

Figure 3. Upper panel: Number of LAEs (N_α) as a function of their Lyα luminosity (L_α) in the COSMOS/UDS/SA22 fields (Matthee et al. 2015, green pentagons). The histogram shows the predicted number of composite (i.e. Pop III hosts) LAEs in the same survey; the bar colors indicate the expected $L_{\rm HeII}$ emission, also shown by the numbers in the bars. **Lower panel**: Fraction of composite galaxies ($f_\alpha^{\rm comp}$, eq. 2a) for which the correction for the finite volume bias (eq. 2b) of Matthee et al. (2015) survey has been included (red solid) or neglected (black dashed).

$L_\alpha = 10^{43.9}{\rm erg\,s^{-1}}$, with no contribution from clumps B+C ($\rm SFR_2 = 0$). This comparison allows us to determine, using eq. 1b, the Lyα line attenuation factor, $A_\alpha = 10^{-0.57}$.

Roughly 66% of the line luminosity is therefore damped, a figure consistent with other derivations (e.g. Dayal et al. 2008), and with the analysis of S15. The above procedure provides a basis to model Lyα and He II emission for both pure and composite galaxies, assuming that the properties of the Pop III component are similar to those derived from CR7.

3 PREDICTIONS FOR BRIGHT LAES

Starting from the assumption that CR7 is a "typical" composite galaxy, and using $m_{low} = 6.7\,{\rm M_\odot}$ and $A_\alpha = 10^{-0.57}$, we can now predict how many LAEs among those observed by Matthee et al. (2015) are composite galaxies, i.e. contain Pop III stars. The number of LAEs in the COSMOS/UDS/SA22 fields with luminosity L_α is $N_\alpha = \Phi_\alpha(L_\alpha)\,V_{obs}$, where Φ_α is the observed Lyα luminosity function and $V_{obs} = 4.26\times10^6\,{\rm Mpc^3}$ is the observed volume. Among these, a fraction

$$f_\alpha^{\rm comp} = N_{\rm comp}/(N_{\rm comp}+N_{\rm pure}) \qquad (2a)$$

contain Pop III stars, where $N_{\rm comp}$ ($N_{\rm pure}$) is the number of composite (pure) galaxies in V_{obs} at a given L_α.

Eq.s 1a and 1b, show that a given L_α can be produced by a composite galaxy with a lower $M_\star$ with respect to a pure (PopII) galaxy. For instance, $L_\alpha \simeq 10^{43.5}{\rm erg\,s^{-1}}$ requires $M_\star \simeq 10^{10.5}{\rm M_\odot}$ for a pure galaxy, but only $M_\star \lesssim 10^{9.5}{\rm M_\odot}$ for a composite one. Such large objects are very rare at the redshift of CR7 ($z = 6.6$) and in the observed volume[5]. Therefore, it is important to account for the statistical (Poisson) fluctuations of the galaxy number counts as follows:

$$N_\kappa = n_\kappa V_{obs}(1 \pm (n_\kappa V_{obs})^{-1/2}), \qquad (2b)$$

where κ = (composite, pure). The distribution of $n_{\rm comp}(M_\star)$ is shown in the upper panel of Fig. 2 as the "young" Pop III curve[6]; while $n_{\rm pure}$ accounts for the remaining galaxies. The effect of the finite volume effects on $f_\alpha^{\rm comp}$ can be appreciated from the lower panel of Fig. 3. Assuming a higher $\rm sSFR = 5\,Gyr^{-1}$ (e.g. Stark et al. 2013) yields the modifications shown by the dash-dotted line.

In the upper panel of Fig. 3 we plot the LAE number (N_α) as a function of L_α. Matthee et al. (2015) observations (green pentagons) are shown along with our predictions for the composite LAE and expected $L_{\rm HeII}$ emission. CR7 is the most luminous LAE observed, and it is in the brightest luminosity bin ($L_\alpha = 10^{44\pm0.1}{\rm erg\,s^{-1}}$); by assumption CR7 is a composite galaxy. If so, we then predict that out of the 46 (30) LAEs with $L_\alpha = 10^{43.2\pm0.1}{\rm erg\,s^{-1}}$ ($> 10^{43.3}{\rm erg\,s^{-1}}$, cumulative), 13 (14) must also be composite galaxies[7], with observable $L_{\rm HeII} \simeq 10^{42.5}{\rm erg\,s^{-1}}$ ($\gtrsim 10^{42.7}{\rm erg\,s^{-1}}$). Follow-up spectroscopy of those luminous Lyman-α emitters at $z = 6.6$ will allow to test this prediction. We recall that this test assumes that all Pop III give raise to the same Lyα and He II emission as inferred from CR7, that requires that all the Pop III stellar mass was formed in a single burst with age $\lesssim 2$ Myr.

Particularly in the regime where $f_{\rm comp} < 1$ (see lower panel in Fig. 3), a sample of LAEs is needed to test our model predictions. For example for "Himiko", the second most luminous[8] confirmed LAE at $z = 6.6$ with $L_\alpha \simeq 10^{43.4}{\rm erg\,s^{-1}}$ (Ouchi et al. 2009), for which recent VLT/X-Shooter observations have provided a 3σ limit of $L_{\rm HeII} \lesssim 10^{42.1}{\rm erg\,s^{-1}}$ (Zabl et al. 2015), our model predicts $L_{\rm HeII} \simeq 10^{42.7}{\rm erg\,s^{-1}}$ i.e. a four times higher He II luminosity. However, this is predicted only for $f_{\rm comp} \simeq 20-30\%$ of galaxies at this L_α.

4 ALTERNATIVE INTERPRETATION

Given the extreme conditions required to explain the observed properties of CR7 in terms of Pop III stars and a set of assumptions, it is worth exploring alternative interpretations. The most appealing one involves Direct Collapse Black Holes (DCBH), which is briefly discussed in S15. High-z pristine, atomic halos ($M_h \gtrsim 10^8{\rm M_\odot}$) primarily cool via Ly$\alpha$ line emission. In the presence of an intense Lyman-Werner (LW, $E_\gamma = 11.2-13.6\,{\rm eV}$) irradiation, H_2 molecule photo-dissociation enforces an isothermal collapse (Shang

[5] As a reference, a $M_\star \sim 10^{10.5}{\rm M_\odot}$ is hosted in a dark matter halo of mass $M_h \sim 10^{12.5}{\rm M_\odot}$, whose abundance is $n_h \sim 10^{-6}{\rm Mpc^{-3}}$ at $z \simeq 6$ (e.g. Sheth & Tormen 1999).
[6] As noted in Sec. 2.1, all galaxies with $M_\star > 10^7$ have old Pop III stars, thus considering the "old+young" track for $n_{\rm comp}$ would yield an unrealistically high composite number.
[7] The predicted number would become 7 (7), by assuming sSFR from Stark et al. (2013).
[8] As re-computed in S15 using Y band to estimate the continuum, in order to match the calculation for CR7.

et al. 2010; Latif et al. 2013; Agarwal et al. 2013; Yue et al. 2014), finally leading to the formation of a DCBH of initial mass $M_\bullet \simeq 10^{4.5-5.5}\mathrm{M}_\odot$ (Begelman et al. 2006; Volonteri et al. 2008; Ferrara et al. 2014), eventually growing up to $10^{6-7}\mathrm{M}_\odot$ by accretion of the halo leftover gas.

In CR7, clump A appears to be pristine, and it is irradiated by a LW flux from B+C[9] of $\sim 5 \times 10^{-18}\mathrm{erg\,s^{-1}\,cm^{-2}Hz^{-1}\,sr^{-1}}$, well in excess of the required threshold for DCBH formation (Shang et al. 2010; Latif et al. 2013; Sugimura et al. 2014; Regan et al. 2014). Thus CR7 might be a perfect host for a DCBH.

We investigate the time-evolving spectrum of an accreting DCBH of initial mass $M_\bullet = 10^5\mathrm{M}_\odot$ by coupling a 1D radiation-hydrodynamic code (Pacucci & Ferrara 2015) to the spectral synthesis code CLOUDY (Ferland et al. 2013), as detailed in Pacucci et al. (2015). The DCBH intrinsic spectrum is taken from Yue et al. (2013). The DCBH is at the center of a halo of total gas mass $M_g \simeq 10^7\mathrm{M}_\odot$, distributed with a core plus a r^{-2} density profile spanning up to 10 pc. The accretion is followed until complete depletion of the halo gas, i.e. for $\simeq 120$ Myr. During this period the total absorbing column density of the gas varies from an initial value of $\simeq 3.5 \times 10^{24}\mathrm{cm^{-2}}$ to a final value $\ll 10^{22}\mathrm{cm^{-2}}$, i.e. from mildly Compton-thick to strongly Compton-thin. Note that while Lyα attenuation by the interstellar medium is included, we do not account for the likely sub-dominant IGM analogous effect.

Fig. 4 shows the time evolution of the Lyα, He II and X-ray (0.5-2 keV) luminosities. Both Lyα and He II are consistent with the observed CR7 values during an evolutionary phase lasting $\simeq 17$ Myr (14% of the system lifetime), longer than the shorter period ($t_\star \lesssim 2$ Myr) of our assumption for a massive Pop III burst.

The equivalent width of the He II line in the CR7 compatibility region ranges from 75 to 85 A. The column density during the CR7-compatible period is $\simeq 1.7 \times 10^{24}\mathrm{cm^{-2}}$, i.e. mildly Compton-thick. The associated X-ray luminosity is $\lesssim 10^{43}\mathrm{erg\,s^{-1}}$, fully consistent with the current upper limit for CR7 ($\lesssim 10^{44}\mathrm{erg\,s^{-1}}$, Elvis et al. 2009). Deeper X-ray observations of CR7 might then confirm the presence of the DCBH. However, this limit is already obtained with 180 ks of integration time on Chandra, meaning that a stringent test might only be possible with the next generation of X-ray telescopes.

5 CONCLUSIONS

CR7 is the brightest $z = 6.6$ LAE in the COSMOS field (Matthee et al. 2015). Spectroscopic follow-up (Sobral et al. 2015) suggests that CR7 might host Pop III stars, along with Pop II and thus be explained by a "Pop III wave" scenario. We have further investigated such interpretation using cosmological simulations following the formation of Pop II and Pop III stars in early galaxies.

We find simulated galaxies (like MB45 in Fig. 1) hosting both Pop III and Pop II stars at $z = 6.0$. Such "composite" galaxies have morphologies similar to that of CR7 and

[9] The LW is estimated by accounting for the stellar properties of clump B+C (in particular see Fig. 8 in S15), and by assuming a 5 kpc distance between B+C and A.

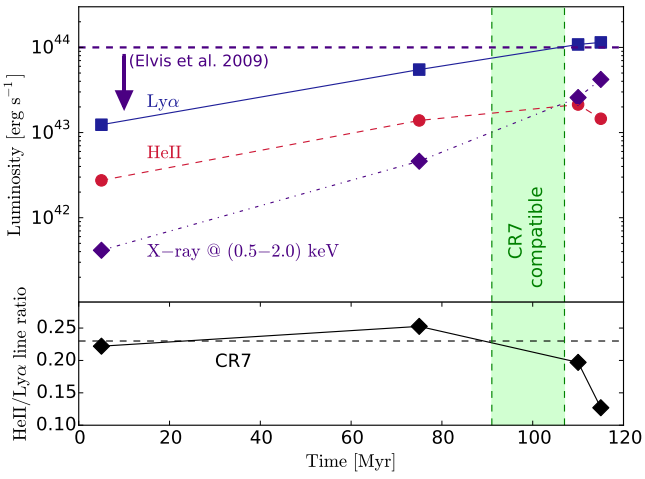

Figure 4. Upper panel: Time evolution of the Lyα (blue solid line), He II (red dashed line) line and X-ray (violet dot dashed line) luminosities calculated for the accretion process onto a DCBH of initial mass $10^5\mathrm{M}_\odot$. The green shaded region indicates the period of time during which our simulations are compatible with CR7 observations. The current upper limit for X-ray is $\lesssim 10^{44}\,\mathrm{erg\,s^{-1}}$, (Elvis et al. 2009, horizontal violet line). **Lower panel**: Time evolution of the HeII/Lyα lines ratio. The black horizontal dashed line indicates the observed values for CR7.

consistent with the "Pop III wave scenario". However, to reproduce the extreme CR7 Lyα/HeII1640 line luminosities, a top-heavy IMF combined with a massive ($M_3 \gtrsim 10^7\mathrm{M}_\odot$) Pop III burst of young stars ($t_\star \lesssim 2-5$ Myr) is required. Our simulations do not predict such large burst, i.e. $M_3 \simeq 10^6\mathrm{M}_\odot$, but our volume is also smaller than that used to discover CR7. Nonetheless, assuming that CR7 is typical of all metal-free components in our simulations, we predict that in the combined COSMOS, UDS and SA22 fields, out of the 30 LAEs with $L_\alpha > 10^{43.3}\mathrm{erg\,s^{-1}}$, 14 should also host Pop III stars producing an observable $L_{\mathrm{HeII}} \gtrsim 10^{42.7}\mathrm{erg\,s^{-1}}$.

Given the extreme requirements set by the Pop III interpretation, we explored the possibility that CR7 is instead powered by accretion onto a Direct Collapse Black Hole (DCBH) of initial mass $10^5\mathrm{M}_\odot$. The predicted L_α and L_{HeII} match CR7 observations during a time interval of ~ 17 Myr ($\sim 14\%$ of the system lifetime). The predicted CR7 luminosity at 0.5-2 keV, $\lesssim 10^{43}\,\mathrm{erg\,s^{-1}}$, is significantly below the current upper limit, i.e. $\lesssim 10^{44}\,\mathrm{erg\,s^{-1}}$.

We conclude that the DCBH interpretation of CR7 is very appealing, and competitive with the explanation involving a massive Pop III burst. For both explanations, the dominant ionizing source of this galaxy should have formed from pristine gas. Deep X-ray observations and other follow-up observations should allow to shed more light on this very peculiar source.

ACKNOWLEDGMENTS

SS acknowledges support from the Netherlands Organization for Scientific research (NWO), VENI grant 639.041.233. RS acknowledges support from the European Research Council under the European Union (FP/2007-

2013)/ERC Grant Agreement n. 306476. D. Sobral acknowledges (i) financial support from the NWO through a Veni fellowship and (ii) funding from FCT through a FCT Investigator Starting Grant and Start-up Grant (IF/01154/2012/CP0189/CT0010) and from FCT grant PEst-OE/FIS/UI2751/2014.

References

Agarwal B., Davis A. J., Khochfar S., Natarajan P., Dunlop J. S., 2013, MNRAS, 432, 3438
Begelman M. C., Volonteri M., Rees M. J., 2006, MNRAS, 370, 289
Bouwens R. J., et al., 2012, ApJ, 754, 83
Brinchmann J., Pettini M., Charlot S., 2008, MNRAS, 385, 769
Bromm V., Coppi P. S., Larson R. B., 2002, ApJ, 564, 23
Cai Z., et al., 2011, ApJL, 736, L28
Cassata P., et al., 2013, A&A, 556, A68
Daddi E., et al., 2007, ApJ, 670, 156
Dayal P., Ferrara A., Gallerani S., 2008, MNRAS, 389, 1683
De Breuck C., Röttgering H., Miley G., van Breugel W., Best P., 2000, A&A, 362, 519
Elvis M., et al., 2009, ApJS, 184, 158
Erb D. K., Pettini M., Shapley A. E., Steidel C. C., Law D. R., Reddy N. A., 2010, ApJ, 719, 1168
Ferland G. J., et al., 2013, Revista Mexicana de Astronomia y Astrofisica, 49, 137
Ferrara A., Salvadori S., Yue B., Schleicher D. R. G., 2014, preprint, (arXiv:1406.6685)
González V., Labbé I., Bouwens R. J., Illingworth G., Franx M., Kriek M., 2011, ApJL, 735, L34
Greif T. H., Bromm V., Clark P. C., Glover S. C. O., Smith R. J., Klessen R. S., Yoshida N., Springel V., 2012, MNRAS, 424, 399
Heap S., Bouret J.-C., Hubeny I., 2015, preprint, (arXiv:1504.02742)
Kashikawa N., et al., 2012, ApJ, 761, 85
Kehrig C., Vílchez J. M., Pérez-Montero E., Iglesias-Páramo J., Brinchmann J., Kunth D., Durret F., Bayo F. M., 2015, ApJL, 801, L28
Larson D., et al., 2011, ApJS, 192, 16
Latif M. A., Schleicher D. R. G., Schmidt W., Niemeyer J. C., 2013, MNRAS, 436, 2989
Ma Q., Maio U., Ciardi B., Salvaterra R., 2015, MNRAS, 449, 3006
Maio U., Ciardi B., Dolag K., Tornatore L., Khochfar S., 2010, MNRAS, 407, 1003
Matthee J., Sobral D., Santos S., Röttgering H., Darvish B., Mobasher B., 2015, MNRAS, 451, 4919
McLure R. J., et al., 2011, MNRAS, 418, 2074
Nagao T., et al., 2008, ApJ, 680, 100
Ouchi M., et al., 2009, ApJ, 696, 1164
Pacucci F., Ferrara A., 2015, MNRAS, 448, 104
Pacucci F., Ferrara A., Volonteri M., Dubus G., 2015, preprint, (arXiv:1506.05299)
Pallottini A., Ferrara A., Gallerani S., Salvadori S., D'Odorico V., 2014a, MNRAS, 440, 2498
Pallottini A., Gallerani S., Ferrara A., 2014b, MNRAS, 444, L105
Pallottini A., Gallerani S., Ferrara A., Yue B., Vallini L., Maiolino R., Feruglio C., 2015, preprint, (arXiv:1506.05803)
Raiter A., Schaerer D., Fosbury R. A. E., 2010, A&A, 523, A64
Regan J. A., Johansson P. H., Wise J. H., 2014, ApJ, 795, 137
Salvadori S., Ferrara A., 2009, MNRAS, 395, L6
Salvadori S., Tolstoy E., Ferrara A., Zaroubi S., 2014, MNRAS, 437, L26
Schaerer D., 2002, A&A, 382, 28
Schneider R., Ferrara A., Natarajan P., Omukai K., 2002, ApJ, 571, 30
Schneider R., Omukai K., Inoue A. K., Ferrara A., 2006, MNRAS, 369, 1437
Shang C., Bryan G. L., Haiman Z., 2010, MNRAS, 402, 1249
Sheth R. K., Tormen G., 1999, MNRAS, 308, 119
Sobral D., Matthee J., Darvish B., Schaerer D., Mobasher B., Röttgering H., Santos S., Hemmati S., 2015, ApJ, 808, 139
Stark D. P., Schenker M. A., Ellis R., Robertson B., McLure R., Dunlop J., 2013, ApJ, 763, 129
Sugimura K., Omukai K., Inoue A. K., 2014, MNRAS, 445, 544
Teyssier R., 2002, A&A, 385, 337
Tornatore L., Ferrara A., Schneider R., 2007, MNRAS, 382, 945
Trenti M., Stiavelli M., Michael Shull J., 2009, ApJ, 700, 1672
Turk M. J., Abel T., O'Shea B., 2009, Science, 325, 601
Visbal E., Haiman Z., Bryan G. L., 2015, preprint, (arXiv:1505.06359)
Volonteri M., Lodato G., Natarajan P., 2008, MNRAS, 383, 1079
Wise J. H., Turk M. J., Norman M. L., Abel T., 2012, ApJ, 745, 50
Xu H., Wise J. H., Norman M. L., 2013, ApJ, 773, 83
Yoshida N., Omukai K., Hernquist L., Abel T., 2006, ApJ, 652, 6
Yue B., Ferrara A., Salvaterra R., Xu Y., Chen X., 2013, MNRAS, 433, 1556
Yue B., Ferrara A., Salvaterra R., Xu Y., Chen X., 2014, MNRAS, 440, 1263
Zabl J., Nørgaard-Nielsen H. U., Fynbo J. P. U., Laursen P., Ouchi M., Kjærgaard P., 2015, MNRAS, 451, 2050
Zheng W., et al., 2012, Nature, 489, 406

This paper has been typeset from a TEX/LATEX file prepared by the author.